

Reach-scale river dynamics moderate the impact of rapid Holocene climate change on floodwater farming in the desert Nile

Mark G. Macklin^{1*}, Jamie C. Woodward^{2*}, Derek A. Welsby³, Geoff A.T. Duller¹, Frances M. Williams⁴, and Martin A.J. Williams⁵

¹Institute of Geography and Earth Sciences, Aberystwyth University, Aberystwyth, SY23 3DB, UK

²School of Environment and Development, The University of Manchester, Manchester, M13 9PL, UK

³Department of Ancient Egypt and Sudan, The British Museum, London, WC1B 3DG, UK

⁴School of Chemistry and Physics, University of Adelaide, Adelaide, SA 5005, Australia

⁵Geography, Environment and Population, University of Adelaide, Adelaide, SA 5005, Australia

*Emails: mvm@aber.ac.uk; jamie.woodward@manchester.ac.uk

Optically Stimulated Luminescence Dating

Ages for deposition of sediments were determined using optically stimulated luminescence (OSL). This method uses quartz grains within sediments as a dosimeter, integrating the radiation dose received during the period of burial (Duller, 2004; Lian and Roberts, 2006). OSL dating of sediments is based on the observation that exposure of mineral grains to daylight rapidly removes the OSL signal, effectively resetting the clock to zero at the time of deposition. After burial the grains are exposed to naturally occurring ionising radiation. In the laboratory, the intensity of the luminescence signal can be used to calculate the equivalent dose (D_e), an estimate of the total radiation dose received since burial. A second set of measurements are made on each sample to assess the rate at which radiation is produced by radionuclides within the sediment and to calculate the contribution of cosmic rays. The age of the sample is calculated by dividing the equivalent dose (D_e) by the radiation dose rate:

$$\text{Age (ka)} = \frac{\text{Equivalent Dose } (D_e, \text{Gy})}{\text{Dose Rate (Gy / ka)}}$$

The reliability of OSL dating of aeolian and fluvially deposited sediments using quartz has been verified in many studies (Murray and Olley, 2002; Roberts, 2008).

Sample collection. Samples were collected in the field by hammering opaque metal tubes into a cleaned sedimentary face. The ends of the tubes were sealed with tape to prevent movement of material within the tubes during transport back to the laboratory (see Woodward et al. 2001). In the laboratory material from each end of the tube was removed. This material may have been exposed to daylight during sample collection and so was not used for OSL measurements. Instead it was used to calculate the dose rate for the samples. The sediment from the centre of the sample tube was used for OSL measurements. It was extracted under red light conditions to avoid damaging the luminescence signal.

Determining the radiation dose rate. The dose rate to the sand-size grains of quartz used in this study originates from beta particles and gamma rays from the surrounding sediment, and cosmic rays. Different methods were used to measure each contribution. After drying, each subsample for dose rate determination was finely milled. One portion of this milled material was used to determine the beta dose rate of the sample using a GM-25-5 beta counter (Bøtter-Jensen and Mejdahl, 1988)). Samples were measured in triplicate, and the beta dose rate calculated by comparison with two reference materials. To determine the gamma dose rate a second subsample was fused with a sodium metaborate flux and put into solution. The resulting solutions were analysed using ICP-OES to determine the concentration of K and ICP-MS to determine the concentration of U and Th. Conversion factors of were then used (Adamiec and Aitken, 1998) to calculate the gamma dose rate.

The beta and gamma dose rates determined above were corrected for the effects of grain size and water content, giving the values shown in Table 1. The contribution of cosmic rays to the overall dose rate was calculated using the equations in (Prescott and Hutton, 1994), taking into account the longitude and latitude of the samples and their burial depth. The cosmic dose rate was combined with the beta and gamma dose rates to give the total dose rate to these samples (Table 1).

All dose rates have been calculated using a water content of $3 \pm 2\%$. This is the value that we think best approximates the "average" conditions during the whole period of burial. This is not straightforward because climate and local hydrology have changed markedly over time. We measured the water content of all OSL samples in the laboratory. All values were very low ($< 1.0\%$) reflecting the present-day hyper-arid climate. It is reasonable to assume that values have been very low since the channels dried out. They would have been much higher of course when the channels were active. We believe that $3 \pm 2\%$ is a fair approximation and this has yielded results that are in good agreement with the four radiocarbon dates (Table 3).

Sample preparation for OSL measurements. The sub-samples for OSL measurement were treated with 10% hydrochloric acid and 20% vols. hydrogen peroxide to remove carbonates and organics. Samples were dried and sieved to obtain grains within a narrow size range, typically 125-180 or 180-211 μm in diameter. Density separation at 2.62 and 2.70 g/cm^3 was undertaken to remove feldspars and heavy minerals. Grains were etched in 40% hydrofluoric acid to remove

any remaining feldspar grains, and to etch away the outer alpha-irradiated skin of the grains. After etching with hydrofluoric acid the grains were immediately washed in hydrochloric acid to prevent the formation of fluoride precipitates and re-sieved to remove any small fragments of feldspar.

Measurement of the equivalent dose. Measurements of the OSL signals from quartz were undertaken in both the Aberystwyth and Adelaide luminescence laboratories (Table 1 and 2). Both laboratories used Risø TL/OSL readers equipped with blue light emitting diodes (LEDs, 470±20 nm) for optical stimulation, and EMI 9635QA photomultiplier tubes (PMTs) to measure the resulting OSL emission. Hoya U-340 filters were placed in front of the PMTs to reject photons from the blue LEDs used for stimulation, but allow the emitted OSL to be transmitted to the PMT. A single aliquot regenerative dose (SAR) protocol (Wintle and Murray, 2006) was used to determine the equivalent dose (D_e) for each aliquot. Figure 1 shows a typical OSL decay curve and dose response curve for a single aliquot. Uncertainties on individual D_e values were determined using a method (Duller, 2007) which incorporates the uncertainty due to counting statistics on each individual OSL decay curve, the uncertainty in the curve fitting procedure, and also a 1.5% uncertainty associated with the Risø instruments used for these measurements. The reliability of the data for individual aliquots was assessed by a number of criteria: 1) recycling ratio between 0.85-1.15 within uncertainty limits; 2) an OSL-IR depletion ratio (Duller, 2003) between 0.9-1.1 within uncertainty limits; 3) a net OSL signal from the test dose that is at least three times larger than the standard deviation of the background; and 4) a dose response curve where the signal increases monotonically with dose.

The comparability of the data sets measured in Aberystwyth and Adelaide was assessed by making replicate measurements in the two laboratories on a sub-set of the samples. Figure 2 shows a radial plot for a typical sample analysed in both laboratories, demonstrating the consistency in measurements.

A number of different types of sediment was analysed in this study including aeolian sands blown into palaeochannels and channels fills. An objective approach was taken to assess whether the distribution of equivalent dose values was consistent with complete removal of trapped charge from the OSL signal at deposition, or whether some residual dose was present. The overdispersion of the equivalent dose values for each sample was calculated (Galbraith et al. 1999). Where the overdispersion was less than 20% this was taken to indicate complete resetting of the OSL at deposition and the central age model (CAM) was used to combine these D_e values to obtain a single value for use in age calculation. For those samples where overdispersion was above 20%, the finite mixture model (FMM) was used to identify the best bleached component within the sample, following a method developed for Holocene fluvial sediments in South Africa (Rodnight et al. 2006). This approach was used by both laboratories, with the exception that the Adelaide laboratory made an initial culling of the data set using Chauvenet's rejection criterion to remove outlying D_e values, but this typically only removed 1 or 2 outlying values. The

resulting D_e values used for age calculation, and the age model used are listed in Table 2, along with the resulting ages, and the dates expressed in years BC or AD.

Table DR1. Sample details and analytical results for OSL samples collected from different palaeochannels

Sample Code ¹	Depth (m)	Beta dose ² (Gy/ka)	Gamma dose ³ (Gy/ka)	Cosmic dose (Gy/ka)	Total dose ² (Gy/ka)
Pit 32: N19° 04' 23.9" E30° 35' 11.6"					
135-NL01	0.22	0.60 ± 0.03	0.29 ± 0.02	0.24 ± 0.03	1.12 ± 0.04
135-NL03	0.46	0.57 ± 0.03	0.41 ± 0.02	0.21 ± 0.02	1.18 ± 0.04
135-NL07	1.23	0.89 ± 0.04	0.47 ± 0.02	0.18 ± 0.02	1.53 ± 0.05
135-NL08	1.62	0.53 ± 0.02	0.29 ± 0.02	0.17 ± 0.02	0.99 ± 0.03
135-NL09	1.92	0.25 ± 0.01	0.13 ± 0.01	0.16 ± 0.02	0.55 ± 0.02
Pit 33: N19° 07' 31.0" E30° 30' 12.9"					
SU811	2.08	0.93 ± 0.04	0.60 ± 0.02	0.16 ± 0.02	1.70 ± 0.05
SU812	2.85	1.00 ± 0.04	0.54 ± 0.02	0.15 ± 0.02	1.69 ± 0.05
Pit 34: N19° 04' 25.3" E30° 35' 01.9"					
SU818	1.17	1.01 ± 0.04	0.58 ± 0.02	0.18 ± 0.02	1.76 ± 0.05
SU815	2.75	0.92 ± 0.04	0.62 ± 0.02	0.15 ± 0.02	1.68 ± 0.05
SU814	3.58	1.04 ± 0.05	0.55 ± 0.02	0.14 ± 0.02	1.73 ± 0.05
SU813	4.40	0.98 ± 0.04	0.51 ± 0.02	0.13 ± 0.02	1.61 ± 0.05
Pit 35: N19° 02' 0.6" E30° 33' 37.8"					
135-NL20/SU820	2.74	0.92 ± 0.04	0.55 ± 0.03	0.15 ± 0.02	1.62 ± 0.05
SU819	3.38	1.10 ± 0.05	0.68 ± 0.04	0.14 ± 0.02	1.92 ± 0.06
Pit 36: N19° 04' 14.0" E30° 33' 52.6"					
135-NL24/SU824	2.50	0.97 ± 0.04	0.58 ± 0.03	0.15 ± 0.02	1.70 ± 0.05
135-NL22/SU822	5.00	0.96 ± 0.04	0.40 ± 0.02	0.12 ± 0.01	1.48 ± 0.05
Pit 37: N19° 02' 51.0" E30° 36' 51.4"					
163-0109	2.25	0.79 ± 0.03	0.68 ± 0.02	0.16 ± 0.02	1.63 ± 0.04
Pit 38: N19° 04' 04.4" E30° 36' 51.6"					
SU904	0.99	0.70 ± 0.03	0.71 ± 0.03	0.19 ± 0.02	1.59 ± 0.04
SU903	1.67	0.33 ± 0.01	0.36 ± 0.01	0.17 ± 0.02	0.86 ± 0.02
SU902	2.20	0.46 ± 0.02	0.41 ± 0.02	0.16 ± 0.02	1.03 ± 0.03
Pit 40: N19° 04' 54.6" E30° 36' 37.4"					
163-1409/SU914	2.72	0.87 ± 0.04	0.58 ± 0.02	0.15 ± 0.02	1.59 ± 0.04
163-1309/SU913	3.35	0.17 ± 0.01	0.19 ± 0.01	0.14 ± 0.02	0.50 ± 0.02
Pit 41 (well shaft): N18° 53' 11.2" E30° 33' 52.3"					
SU915	0.70	0.98 ± 0.04	0.61 ± 0.02	0.20 ± 0.02	1.78 ± 0.05
Pit 42 (well shaft): N18° 53' 9.0" E30° 33' 51.6"					
SU916	0.70	1.01 ± 0.04	0.58 ± 0.02	0.20 ± 0.02	1.79 ± 0.05

Notes:

1. Samples prefixed with 135- and 163- were measured in the Aberystwyth Luminescence Research Laboratory, while those prefixed with SU were measured in the Adelaide Luminescence laboratory.
2. All dose rates have been calculated using a water content of 3±2%
3. Conversion factors of Adamiec and Aitken (1998) have been used to calculate the gamma dose rate based on ICP-AES and ICP-MS analyses for K, U and Th.

Table DR2. Sample details and analytical results for OSL samples collected from different palaeochannels

Sample Code	Depth (m)	Grain size (μm)	Number of aliquots ¹	Age Model	D _e (Gy)	Age (ka) ²	Date
Pit 32: N19° 04' 23.9" E30° 35' 11.6"							
135-NL01	0.22	180-212	28(48)	FMM	1.93 ± 0.08	1.73 ± 0.09	280 AD ± 90
135-NL03	0.46	180-212	42(48)	FMM	2.43 ± 0.09	2.05 ± 0.10	45 BC ± 100
135-NL07	1.23	150-212	47(48)	FMM	4.19 ± 0.19	2.74 ± 0.15	730 BC ± 150
135-NL08	1.62	180-212	41(48)	CAM	2.75 ± 0.09	2.79 ± 0.13	780 BC ± 130
135-NL09	1.92	150-212	41(48)	FMM	1.80 ± 0.05	3.30 ± 0.16	1290 BC ± 160
Pit 33: N19° 07' 31.0" E30° 30' 12.9"							
SU811	2.08	125-180	12(20)	FMM	10.0 ± 0.60	5.89 ± 0.39	3880 BC ± 390
SU812	2.85	125-180	28(40)	FMM	10.0 ± 0.34	5.93 ± 0.27	3920 BC ± 270
Pit 34: N19° 04' 25.3" E30° 35' 01.9"							
SU818	1.17	125-180	25(40)	FMM	5.87 ± 0.44	3.33 ± 0.27	1320 BC ± 270
SU815	2.75	125-180	18(25)	FMM	6.17 ± 0.27	3.67 ± 0.19	1660 BC ± 190
SU814	3.58	125-180	28(40)	CAM	6.37 ± 0.19	3.67 ± 0.15	1670 BC ± 150
SU813	4.40	125-180	39(48)	FMM	6.10 ± 0.22	3.79 ± 0.18	1790 BC ± 180
Pit 35: N19° 02' 0.6" E30° 33' 37.8"							
135-NL20/SU820	2.74	180-212	56/29	CAM	7.69 ± 0.14	4.74 ± 0.17	2730 BC ± 170
SU819	3.38	125-180	17(45)	CAM	9.06 ± 0.48	4.73 ± 0.29	2720 BC ± 290
Pit 36: N19° 04' 14.0" E30° 33' 52.6"							
135-NL24/SU824	2.50	125-180	58/30	CAM	6.79 ± 0.15	4.00 ± 0.15	1990 BC ± 150
135-NL22/SU822	5.00	180-212	64/30	CAM	6.12 ± 0.12	4.14 ± 0.15	2130 BC ± 150
Pit 37: N19° 02' 51.0" E30° 36' 51.4"							
163-0109/SU901	2.25	180-212	21/36	CAM	8.30 ± 0.23	5.09 ± 0.19	3080 BC ± 190
Pit 38: N19° 04' 04.4" E30° 36' 51.6"							
SU904	0.99	125-180	23(48)	FMM	8.59 ± 0.34	5.39 ± 0.26	3380 BC ± 260
SU903	1.67	125-180	19(48)	FMM	6.59 ± 0.28	7.69 ± 0.38	5680 BC ± 380
SU902	2.20	125-180	16(48)	FMM	6.44 ± 0.32	6.23 ± 0.35	4220 BC ± 350
Pit 40: N19° 04' 54.6" E30° 36' 37.4"							
163-1409/SU914	2.72	180-212	23/38	FMM	8.87 ± 0.20	5.58 ± 0.19	3570 BC ± 190
163-1309/SU913	3.35	180-212	14/24	FMM	4.20 ± 0.12	8.42 ± 0.33	6410 BC ± 330
Pit 41 (well shaft): N18° 53' 11.2" E30° 33' 52.3"							
SU915	0.70	125-180	34(48)	CAM	5.66 ± 0.14	3.18 ± 0.12	1170 BC ± 120
Pit 42 (well shaft): N18° 53' 9.0" E30° 33' 51.6"							
SU916	0.70	125-180	31(48)	FMM	6.17 ± 0.18	3.45 ± 0.14	1440 BC ± 140

Notes:

1. The number of aliquots accepted after application of rejection criteria and used for D_e calculation. The value in parentheses is the total number of aliquots measured. For samples analysed in both laboratories the number of accepted aliquots is given (e.g. 56/29 means 56 aliquots from Aberystwyth and 29 from Adelaide). In these cases the two sets of D_e were combined.
2. Ages are calculated in ka relative to AD2008 for samples in Pits 32-36, and relative to AD2010 for samples in Pits 37-40

TableDR 3. Radiocarbon dates from the alluvial record in the NDR. All samples were calibrated using the latest OxCal 4.1 program with the calibration curve of Bronk Ramsey (2009).

Sample Code	Location	Depth	Radiocarbon age	Calibrated Age
Beta 100605	Pit 12	1.83 m	5100 ± 80	4050 to 3700 cal BC
BM-3128	Pit 26	1.20 m	3830 ± 50	2460 to 2140 cal BC
Beta 240783	Pit 36	0.25 m	3930 ± 40	2570 to 2290 cal BC
Beta 339076	Pit 40	0.90 m	4980 ± 30	3910 to 3660 cal BC

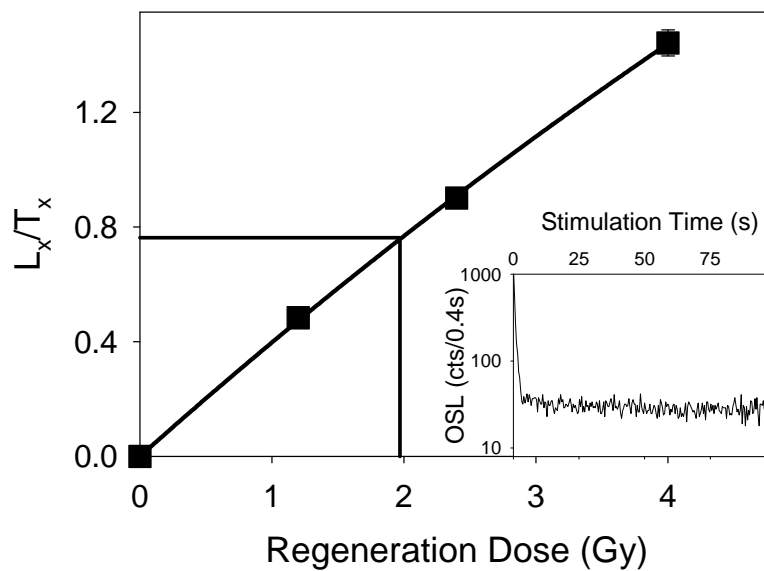


Figure DR1. An example of a dose response for one aliquot of sample 135/NL-07. The equivalent dose for this aliquot is 1.97 Gy. The inset shows the natural OSL decay curve measured from this aliquot.

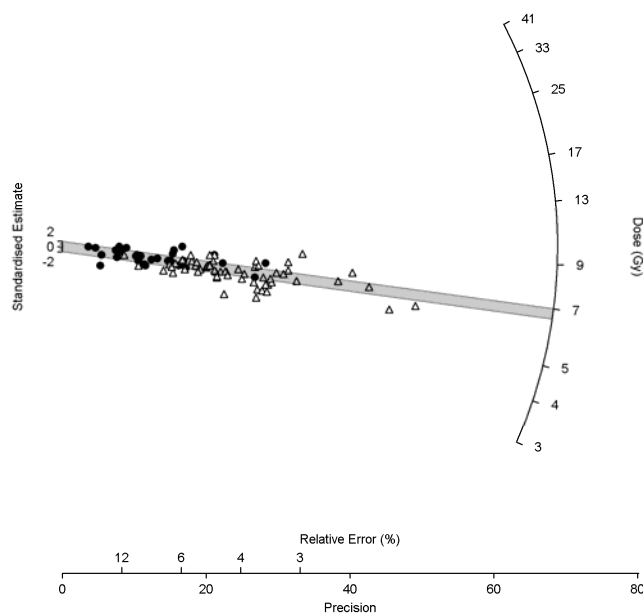


Figure DR2. A radial plot of equivalent dose values obtained for sample 135-NL24/SU824. Open triangles were measured in the Aberystwyth Luminescence Research Laboratory, and filled circles were measured in the luminescence laboratory in Adelaide.

References

- Adamiec G. and Aitken M.J. 1998, Dose-rate conversion factors: An update. *Ancient TL*, v. 16, p. 37–50.
- Bøtter-Jensen L. and Mejdahl V. 1988, Assessment of beta dose-rate using a GM multi-counter system. *Nuclear Tracks and Radiation Measurements*, v. 14, p. 187–191.
- Bronk Ramsey, C. (2009). Bayesian analysis of radiocarbon dates. *Radiocarbon*, v. 51, p. 337–360.
- Duller G.A.T. 2004, Luminescence dating of Quaternary sediments: recent advances. *Journal of Quaternary Science*, v. 19, p. 183–192.
- Duller G.A.T. 2003, Distinguishing quartz and feldspar in single grain luminescence measurements. *Radiation Measurements*, v. 37, p. 161–165.
- Duller G.A.T. 2007, Assessing the error on equivalent dose estimates derived from single aliquot regenerative dose measurements. *Ancient TL*, v. 25, p. 15–24.
- Galbraith R.F., Roberts R.G., Laslett G.M., Yoshida H., Olley J.M. 1999, Optical dating of single and multiple grains of quartz from Jinmium rock shelter, northern Australia: Part I, Experimental design and statistical models. *Archaeometry*, v. 41, p. 339–364.
- Lian O.B. and Roberts, R.G. 2006, Dating the Quaternary: progress in luminescence dating of sediments. *Quaternary Science Reviews*, v. 25, p. 2449–2468.

Murray, A.S. and Olley J.M. 2002, Precision and accuracy in the optically stimulated luminescence dating of sedimentary quartz: a status review. *Geochronometria*, v. 21, p. 1–16.

Prescott J.R. and Hutton J.T. 1994, Cosmic ray contributions to dose rates for luminescence and ESR dating: large depths and long-term time variations. *Radiation Measurements*, v. 23, p. 497–500.

Roberts H.M. 2008, The development and application of luminescence dating to loess deposits: a perspective on the past, present, and future. *Boreas*, v. 37, p. 483–507.

Rodnight H., Duller G.A.T., Wintle A.G., Tooth S. 2006, Assessing the reproducibility and accuracy of optical dating. *Quaternary Geochronology*, v. 1, p. 109–12.

Wintle A.G. and Murray A.S. 2006, A review of quartz optically stimulated luminescence characteristics and their relevance in single-aliquot regeneration dating protocols. *Radiation Measurements*, v. 41, p. 369–391.

Woodward, J C., Macklin, M.G. and Welsby, D.A. 2001, The Holocene fluvial sedimentary record and alluvial geoarchaeology in the Nile Valley of Northern Sudan, *in* Maddy, D.M., Macklin, M.G. and Woodward, J.C ed., *River Basin Sediment Systems: Archives of Environmental Change*: Abingdon, Balkema, p. 327-356.